

**EFFECT OF EXTREME TEMPERATURE
THERMAL CYCLING OF 8-PIN PLASTIC DIP-
PACKAGE ANALOG DEVICES OP181 GP
OPERATIONAL AMPLIFIERS**

Richard Patterson¹, Scott Gerber², Ahmad Hammoud³
Rajeshuni Ramesham⁴, Reza Ghaffarian⁴, and Michael Newell⁴

¹NASA Glenn Research Center, Cleveland, OH

²ZIN Technologies, NASA Glenn Research Center, Cleveland, OH

³QSS Group Inc., NASA Glenn Research Center, Cleveland, OH

⁴Jet Propulsion Laboratory, California Institute of Technology, Pasadena, CA

EFFECT OF EXTREME TEMPERATURE THERMAL CYCLING OF 8-PIN PLASTIC DIP-PACKAGE ANALOG DEVICE OP181 GP OPERATIONAL AMPLIFIERS

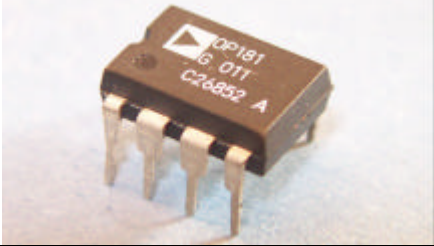
Introduction

The Analog Devices OP181 GP is an ultra-low power operational amplifier featuring rail-to-rail output. It requires less than 4 μ A of quiescent current and employs a bipolar differential pair in its input stage [1]. The output stage consists of a pair of CMOS transistors in a common source configuration. The device operates from supplies as low as 2 V and is specified at +3 V and +5 V single supply as well as \pm 5 V dual supplies. The operating temperature limits of these parts is specified between -40°C and $+85^{\circ}\text{C}$, and the devices are typically used in battery and power supply control, signal conditioning, remote sensing, and transducer interface in very low power systems.

Experimental Test Setup

Two circuit boards, each populated with an OP181 GP, and a few passive components (ceramic capacitors and metal film resistors), which were designed in an inverting amplifier configuration, were evaluated in the temperature range of $+90^{\circ}\text{C}$ to -185°C . Each OP181 GP device, which had an 8-pin plastic DIP package, was inserted into an IC socket on the circuit board. An optical photograph of the chip along with some of the manufacturer's specified properties are shown in Table I [1]. Figure 1 shows a photograph of one of the circuit boards. The industrial-grade parts were evaluated for packaging durability and electrical performance of the devices. The electrical properties, which included signal gain and phase shift, were measured as a function of temperature in the frequency range of 1 kHz to 1 MHz. At each test temperature, the devices were allowed to soak for 15 minutes before any measurements were made. A digital oscilloscope, LeCroy LT374, was used to capture the waveforms of the input and output signals of the inverting amplifier.

Table I. The 8-pin plastic DIP-package OP 181 chip with selected properties.

OP181 IC		
Parameter	Symbol	Value
Input Bias Current	I_B	3 – 10 nA
Input Voltage	I_V	0 – 2 V
Slew Rate	SR	25 V/ms
Turn On Time	$\hat{\delta}_{ON}$	40 – 50 μ s
Gain Bandwidth Product	GBP	95 kHz
Phase Margin	\hat{O}_O	70 degrees

Limited thermal cycling, a total of 60 cycles, was performed on the OP181 GP devices. These tests consisted of initially subjecting the two devices to 10 thermal cycles in the temperature range between +90 °C and -185 °C with a ramp rate of 10°C/min. This was then followed by 50 cycles between +115 °C and -120 °C. A temperature ramp rate of 5 °C/min was used during this thermal cycling step. The temperature profile used to perform 50 thermal cycles is shown in Figure 2. Physical inspection, electrical characterization, and Fein focus X-ray imaging of these packages were performed before and after completion of the thermal cycling.

Results and Discussion

As was mentioned earlier, two devices of OP181 GP amplifiers were investigated in this work. The data obtained on both devices were very similar; therefore, the results of only one device are presented in this report.

Experimental Results:

Microscopic/optical examination and Fein focus x-ray imaging were performed on the two devices before and after thermal cycling. These investigations were performed after the first thermal cycling run (10 cycles between +90 °C and -185 °C), and also after the second thermal cycling run (50 cycles between +115 °C and -120 °C). All of these tests have revealed no evidence of layer delamination, surface and internal cracking, connection breakage, or external solder joint fatigue for either device. X-Ray images of the OP 181 GP device, before and after the thermal cycling, are shown in Figures 3 and 4, respectively. It is evident, from the optical and x-ray images that the exposure to extreme temperatures (namely +115 °C and -185 °C), and thermal cycling (a total of 60 cycles) did not produce any effect either on the devices' material or on their package integrity.

Electrical Performance

Figure 5 shows the gain of the amplifier at various test temperatures in the frequency range of 1 kHz to 1 MHz. At 25 °C, the roll-off frequency, which corresponds to a gain of -3 dB, occurs at about 8 kHz. It can be seen that while the gain remains unaffected with increase in temperature to +90 °C, it changes significantly as the temperature is decreased. This is evident from the gradual drop in the roll-off frequency as the test temperature is decreased. At -170 °C, for example, the roll-off frequency occurs at about 2.5 kHz.

The effect of temperature on the phase shift property of the amplifier seems to have the same trend observed on its gain. Once again, the temperature-induced changes appear only at the low-test temperatures, as shown in Figure 6.

The amplifier's gain as a function of frequency at test temperatures of 90°C, 25 °C, -125 °C, -170 °C, and -185 °C is shown in Figure 7. The depicted results represent those obtained before as well as after the thermal cycling, including those of post 10 and post 60 cycles. It can be seen that the gain of the amplifier exhibits a slight decrease upon subjecting the device to thermal cycling. The reduction experienced in the signal's gain seems to magnify as more cycling is applied, i.e. at 60 cycles. This behavior in the gain was evident at any given test temperature, as shown in Figure 7. Similarly, the phase shift undergoes some changes due to thermal cycling, as shown in Figure 8. These changes are more apparent at the extreme low temperatures, i.e. -170 °C and -185 °C, where the phase shifts by as much as 40 degrees.

Waveforms of the input and the output signals of the amplifier at 1 kHz frequency are depicted at various temperatures in Figure 9. These waveforms were obtained, at a given test temperature, before and after the thermal cycling, as shown in Figures 9a and 9b, respectively. With the exception of $-185\text{ }^{\circ}\text{C}$, the amplifier's signals did not change, in either shape or amplitude, with temperature. Such was the case for before and after the cycling activity. At the lowest test temperature, i.e. $-185\text{ }^{\circ}\text{C}$, the output signal of the amplifier, however, exhibited slight alteration only in its shape while retaining its magnitude. This behavior in signal distortion was observed regardless of the thermal cycle stressing.

At high frequencies, the output signal seemed to undergo shape distortion and a reduction in its magnitude. For example, the waveforms of the input and the output signals of the amplifier obtained at a frequency of 10 kHz are depicted in Figure 10 for various temperatures. The amplitude of the output signal, in particular, decreased as temperature decreased. The effect of temperature at high frequencies was the same for both the pre- as well as the post-thermal cycling conditions. These temperature-induced changes in the device properties were transitory in nature as the amplifier fully recovered to its original characteristics when they were re-tested at room temperature.

Conclusions

Two devices of Analog Devices OP181 GP operational amplifier have been evaluated for potential use in low temperature for space applications (such as Mars, Asteroids, etc). These devices, which were 8-pin plastic DIP packages, were industrial grade with a specified operating temperature from $-40\text{ }^{\circ}\text{C}$ to $+85\text{ }^{\circ}\text{C}$. The devices were characterized for physical integrity and packaging reliability under exposure to extreme temperature thermal cycling. Electrical evaluation in terms of signal gain and phase shift was also carried out in the temperature range of $+90\text{ }^{\circ}\text{C}$ to $-185\text{ }^{\circ}\text{C}$. Limited thermal cycling was also performed on the two devices. The results from this work indicate that these devices experienced no physical degradation with regard to wire bonds, the internal material used by these devices or their exterior packaging, and therefore, the devices may be capable of operation at extreme low temperatures beyond their manufacturer's specification ($-40\text{ }^{\circ}\text{C}$). Although the present work has shown good operational behavior of these devices with temperature down to about $-170\text{ }^{\circ}\text{C}$, further testing and long-term cycling would be needed, however, to fully characterize their performance and to determine their reliability for use in low temperature environments specified for individual missions.

References

[1]. Analog Devices, Inc., OP181 Amplifier Data Sheet, Rev. 0, 1996.

Acknowledgments

This work was performed under the NASA Glenn Research Center, GESS Contract # NAS3-00145, and the Cold Electronics Interconnect Reliability Task at JPL/Caltech. Funds for the work were provided by the NASA Electronic Parts and Packaging (NEPP) Program under Code AE. Our thanks are due to Dr. Charles Barnes and Mr. Phil Zulueta for their interest in this research and evaluation activity.

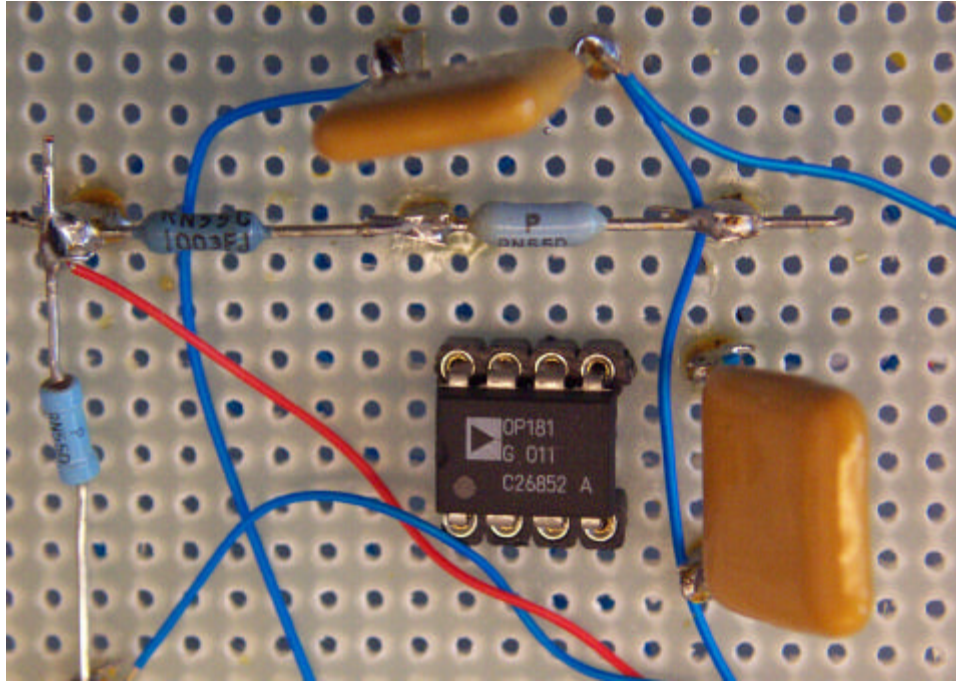


Figure 1: OP181 GP Test Circuit Board.

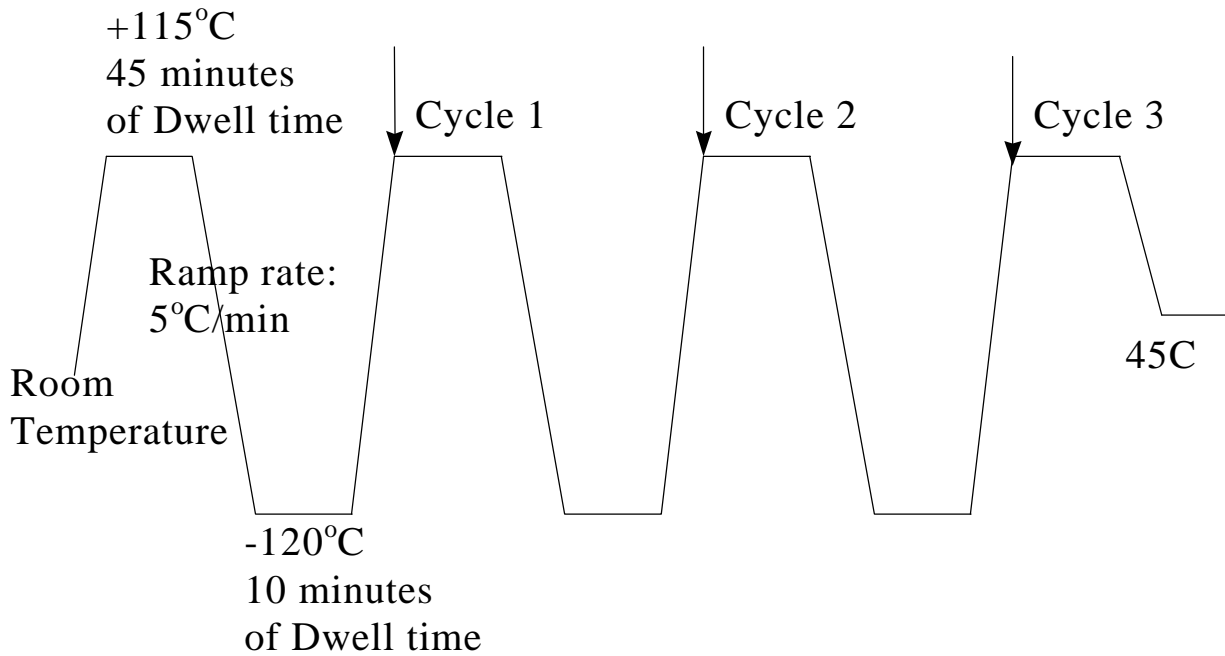


Figure 2: Thermal profile to perform thermal cycling

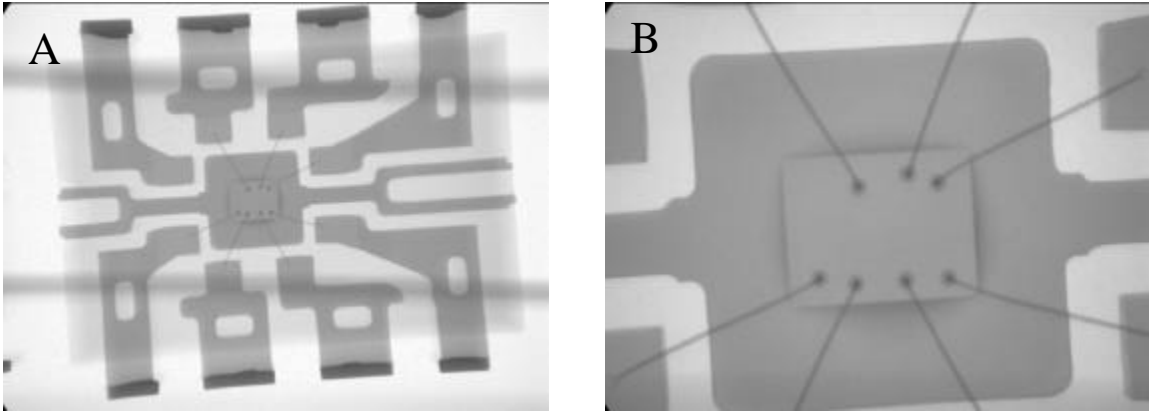


Figure 3. X-Ray images of the OP181 GP prior to thermal cycling.

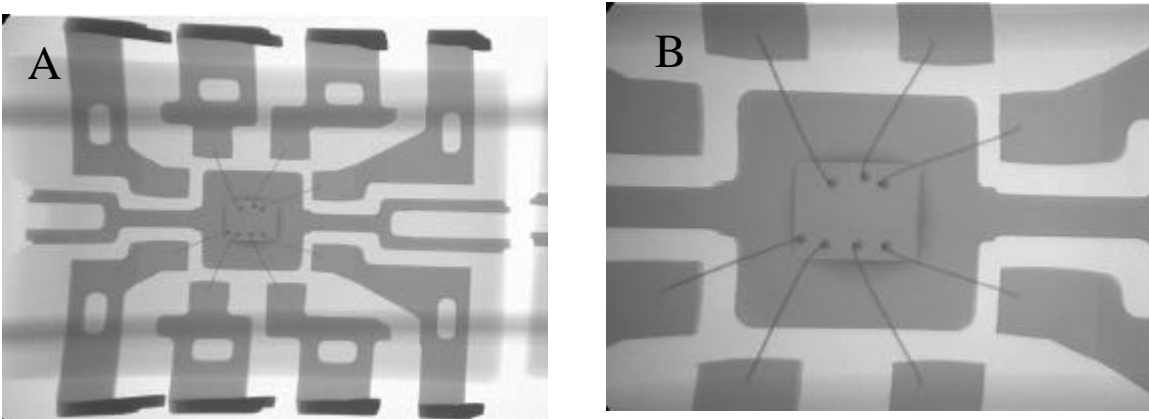


Figure 4. X-Ray images of the OP181 GP after thermal cycling.

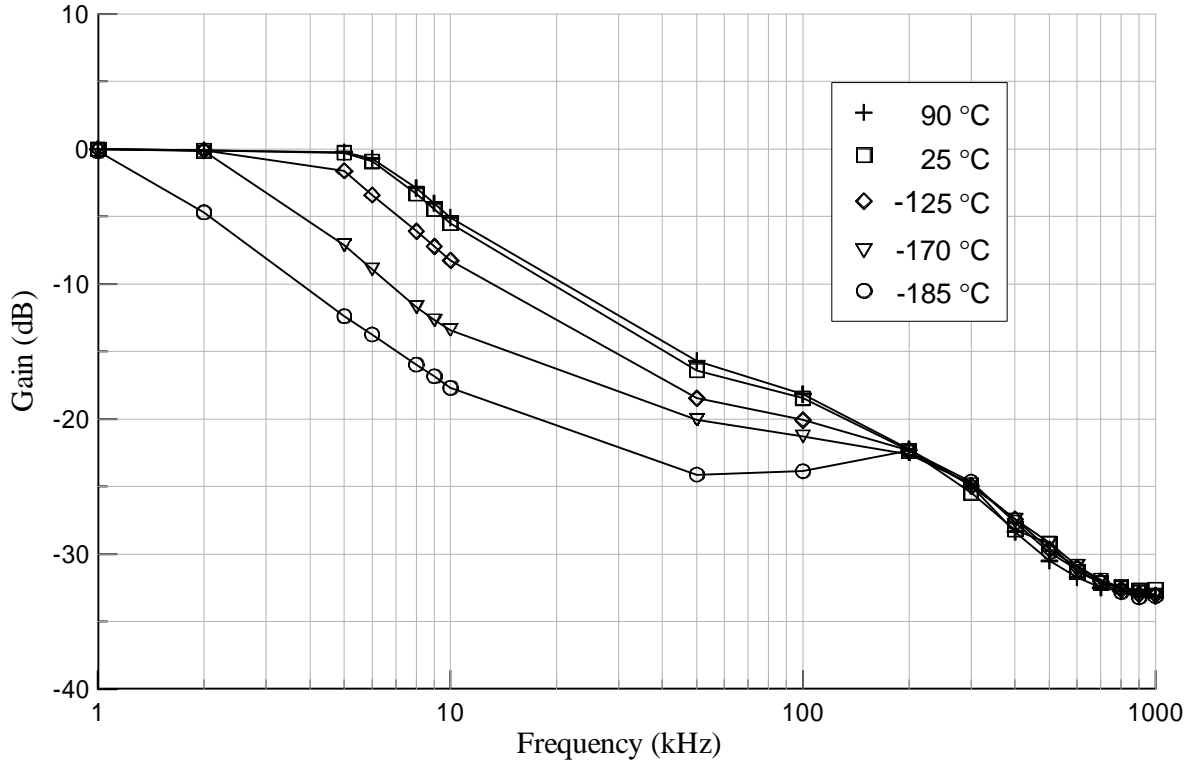


Figure 5. Gain versus frequency at various temperatures.

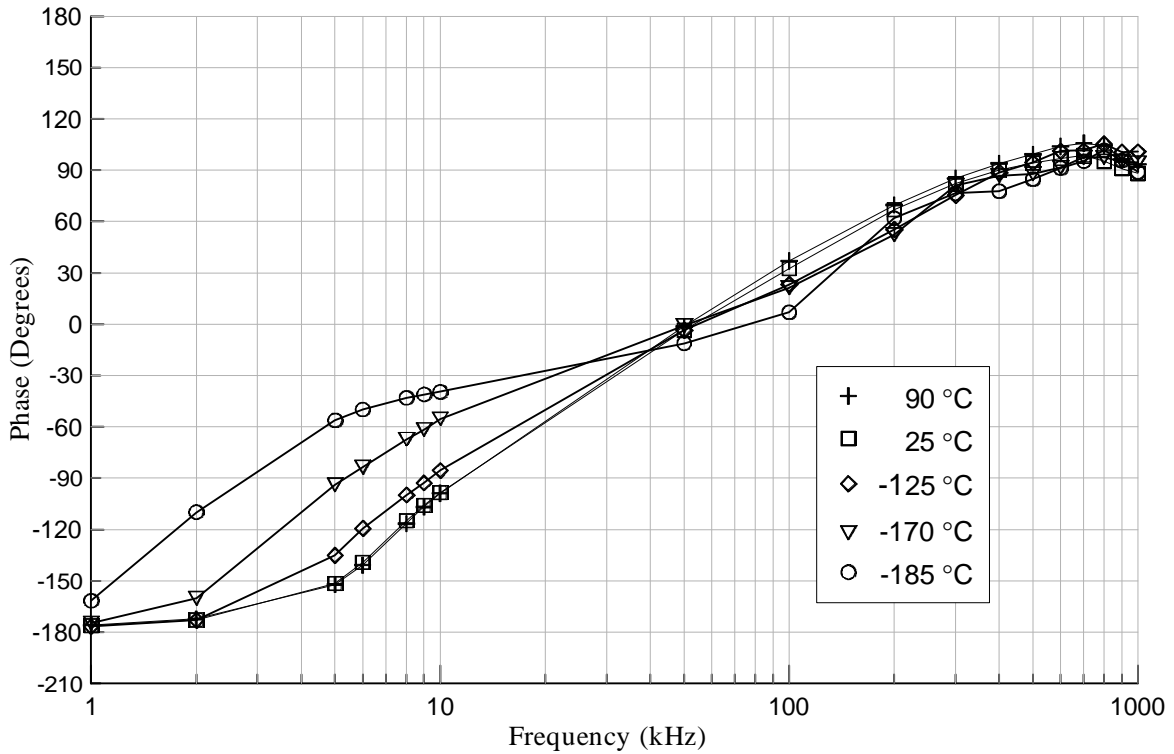


Figure 6. Phase shift versus frequency at various temperatures.

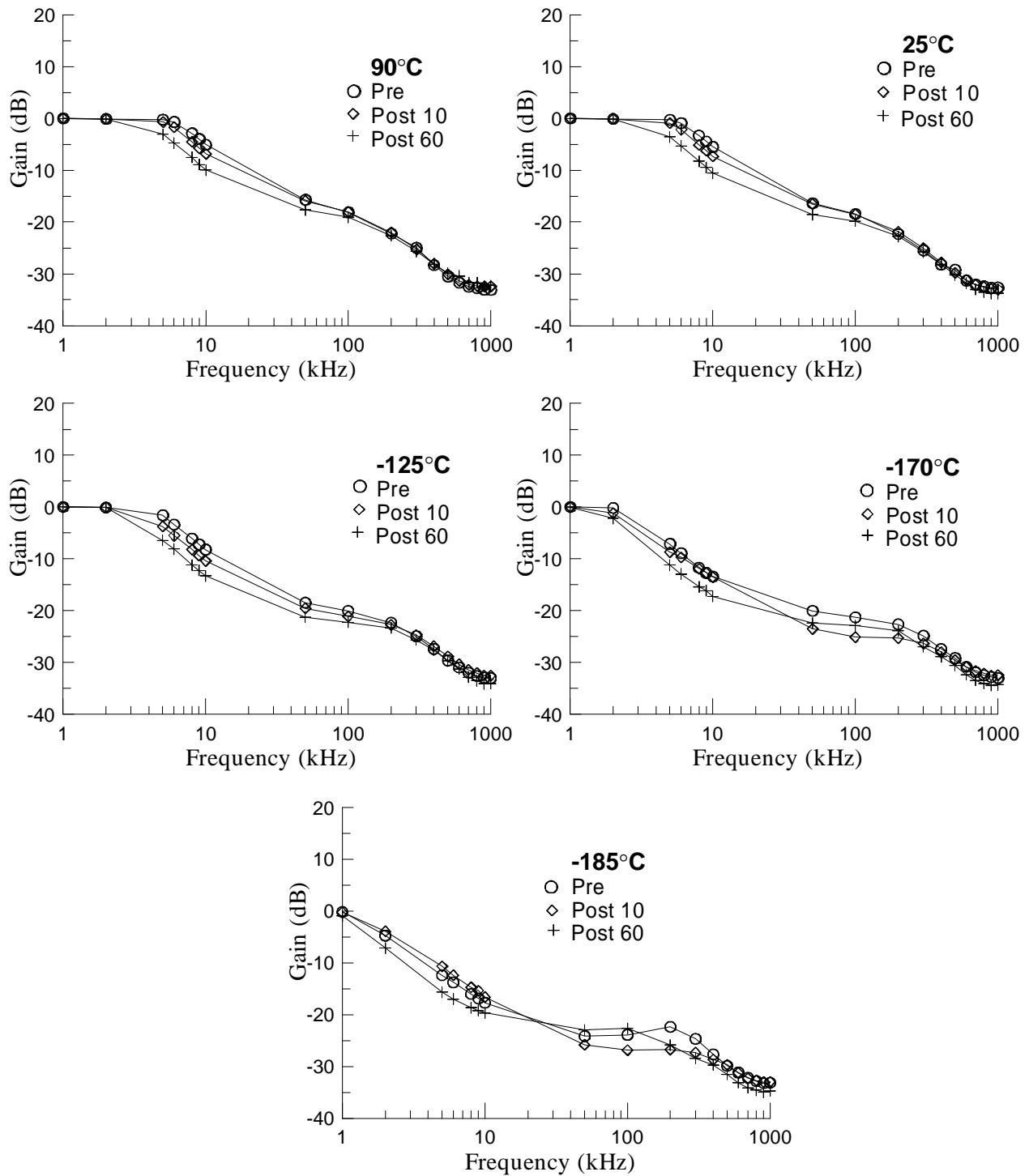


Figure 7. Pre- and post-cycling characteristics of gain versus frequency at various temperatures.

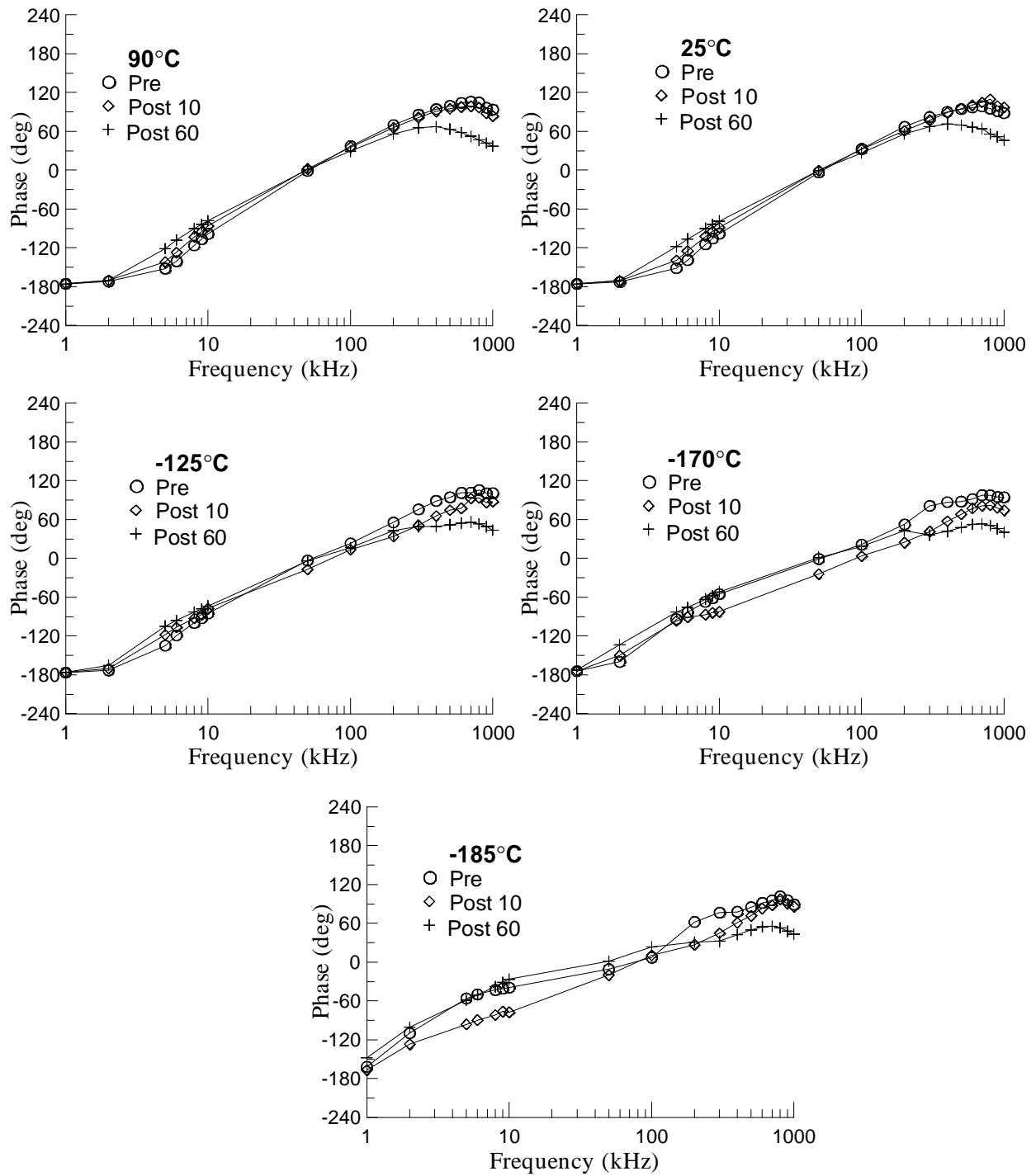


Figure 8. Pre- and post-cycling characteristics of phase versus frequency at various temperatures.

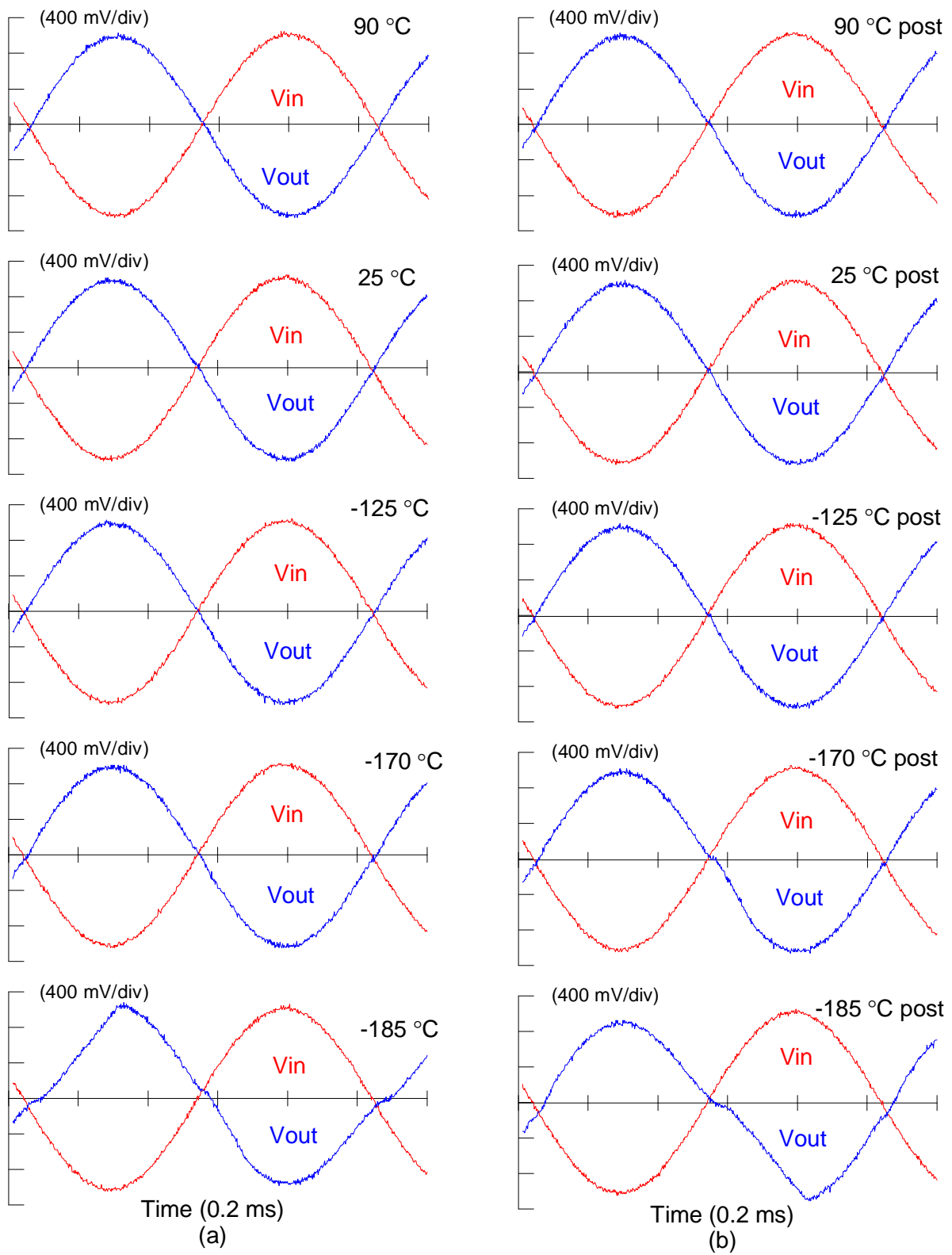


Figure 9. Waveforms of input and output signals at 1 kHz at various temperatures. (a: pre-cycling; b: post-cycling)

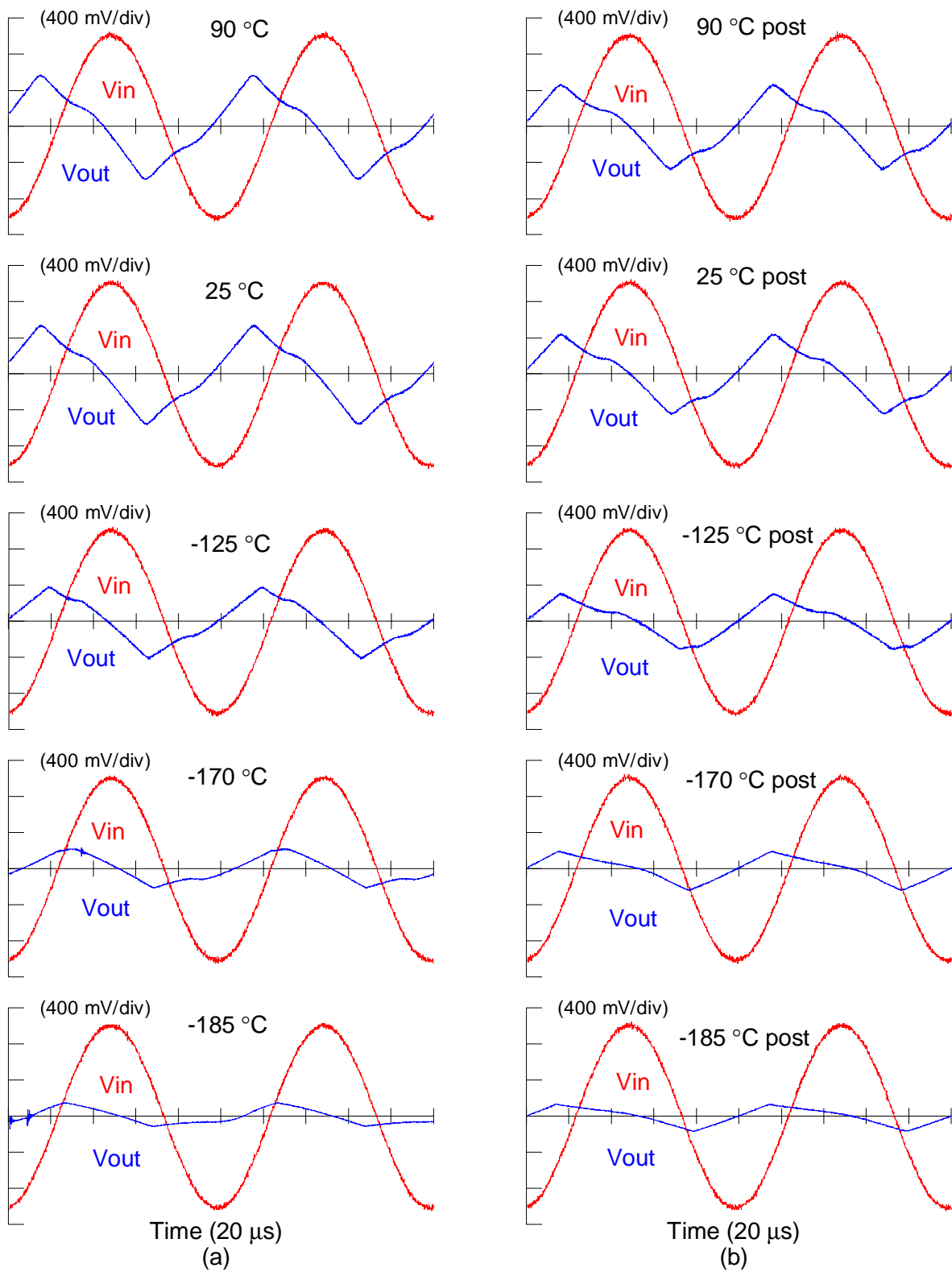


Figure 10. Waveforms of input and output signals at 10 kHz at various temperatures. (a: pre-cycling; b: post-cycling)